ISSN 1070-3284, Russian Journal of Coordination Chemistry, 2013, Vol. 39, No. 6, pp. 463–470. © Pleiades Publishing, Ltd., 2013.
Original Russian Text © O.V. Loseva, T.A. Rodina, A.V. Ivanov, 2013, published in Koordinatsionnaya Khimiya, 2013, Vol. 39, No. 6, pp. 361–369.

A Fixation Mode of Gold(III) in the $[Zn_2\{S_2CN(iso\text{-}C_3H_7)_2\}_4]$–$[AuCl_4]^-$/2 M HCl Chemisorption System: Supramolecular Structure and Thermal Behavior of the Heteropolynuclear Complex $([H_3O][Au_3\{S_2CN(iso\text{-}C_3H_7)_2\}_6][ZnCl_4]_2 \cdot H_2O)_n$

O. V. Loseva[a], T. A. Rodina[b], and A. V. Ivanov[a, *]

[a] *Institute of Geology and Nature Management, Far East Branch, Russian Academy of Sciences, Blagoveshchensk, 675000 Russia*

[b] *Amur State University, Blagoveshchensk, 675027 Russia*

* *e-mail: alexander.v.ivanov@chemist.com*

Received November 7, 2012

Abstract—The interaction of freshly precipitated binuclear zinc dithiocarbamate $[Zn_2\{S_2CN(iso\text{-}C_3H_7)_2\}_4]$ with solutions of $AuCl_3$ in 2 M HCl is studied. The heterogeneous reaction includes the chemisorption of gold(III) and the partial ion exchange to form a polynuclear ionic gold(III)–zinc complex. The molecular and supramolecular structures of the individual fixation mode of gold(III), coordination compound $(H_3O[Au_3\{S_2CN(iso\text{-}C_3H_7)_2\}_6][ZnCl_4]_2 \cdot H_2O)_n$ (**I**), are determined by X-ray diffraction analysis. Compound **I** includes three complex cations $[Au\{S_2CN(iso\text{-}C_3H_7)_2\}_2]^+$, two of which (noncentrosymmetric, A) are structurally nonequivalent with respect to the third cation (centrosymmetric, B). The structural self-organization of compound **I** includes the formation of linear trinuclear fragments $[Au_3\{S_2CN(iso\text{-}C_3H_7)_2\}_6]^{3+}$ by three cations (2A and B) due to nonsymmetric secondary Au···S bonds. The interaction between the $[Au_3\{S_2CN(iso\text{-}C_3H_7)_2\}_6]^{3+}$ fragments results in the formation of zigzag polymer chains $([Au_3\{S_2CN(iso\text{-}C_3H_7)_2\}_6]^{3+})_n$. The outer-sphere water molecule and the hydronium ion are involved in the pairwise linkage of the $[ZnCl_4]^{2-}$ anions due to hydrogen bonds Cl···O. The chemisorption capacity of the zinc dithiocarbamate complex calculated from the reaction of gold(III) fixation is 471.2 mg of gold per 1 g of the sorbent. The conditions for the isolation of chemisorbed gold are determined by the simultaneous thermal analysis of the thermal behavior of compound **I**. The multistage thermal destruction includes two steps of dehydration of the complex, the thermolysis of the dithiocarbamate moiety and $[ZnCl_4]^{2-}$ (with the release of metallic gold and zinc chloride and the partial formation of ZnS), and the evaporation of $ZnCl_2$. The final products of the thermal transformations are metallic gold and ZnS.

DOI: 10.1134/S1070328413050060

INTRODUCTION

Recent studies showed that dithiocarbamate complexes can be interesting as promising sorbents for the concentrating and extraction of noble metals from solutions. We have earlier [1–9] studied the chemisorption properties of the cadmium dialkyl dithiocarbamate complexes towards gold(III) solutions in 2 M HCl in a wide concentration range. Both the heteropolynuclear gold(III)–cadmium complex and polynuclear gold(III) complexes were preparatively isolated from the chemisorption systems at different stages of saturation. The unusually complicated supramolecular structures and properties of these complexes were established by the X-ray diffraction, MAS NMR (^{13}C, ^{15}N, and ^{113}Cd), and simultaneous thermal analysis (STA) data. However, in the most part of cases, gold fixation is accompanied by the escape of toxic cadmium to the solution, which is a substantial drawback of the discussed sorbents.[1] Therefore, it was of interest to study the chemisorption interaction of the zinc dithiocarbamate complexes with gold(III) and to reveal polynuclear complexes as individual fixation modes of gold.

In this work, we studied the interaction of the freshly precipitated binuclear zinc diisopropyl dithiocarbamate (Dtc) complex, $[Zn_2\{S_2CN(iso\text{-}C_3H_7)_2\}_4]$

[1] The exceptions are two compounds that bind gold by a special fixation mode, because this fixation is not accompanied by cadmium escape to the solution due to the formation of hexachlorodicadmate ions: $[Cd_2(S_2CNR_2)_4] + 2H[AuCl_4] = [Au(S_2CNR_2)_2][Cd_2Cl_6] + 2HCl$ ($R = C_2H_5$ [9], C_3H_7 [1]). This reaction is reduced to the addition of two molecules of gold(III) chloride by each binuclear molecule of the complex chemisorbent with the entire ligand redistribution between three coordination spheres.

(chemisorbent), with solutions of $H[AuCl]_4$ in 2 M HCl and preparatively isolated the individual fixation mode of gold(III) from solutions. The binding of gold(III) caused by chemisorption combined with the partial ion exchange affords the polymer heteropolynuclear gold(III)–zinc complex ($H_3O[Au_3\{S_2CN(iso\text{-}C_3H_7)_2\}_6][ZnCl_4]_2 \cdot H_2O)_n$ (**I**). The molecular and supramolecular structures of hydrated complex **I** were determined by X-ray diffraction analysis. The synthesized compound includes two types of isomeric cations (conformers) $[Au\{S_2CN(iso\text{-}C_3H_7)_2\}_2]^+$ in a ratio of 1 : 2. Two noncentrosymmetric (A) and one centrosymmetric (B) complex gold(III) cations are joined by pairs of secondary Au···S bonds to form the linear trinuclear $[Au_3\{S_2CN(iso\text{-}C_3H_7)_2\}_6]^{3+}$ fragment. The adjacent trinuclear fragments are additionally bound by pairs of symmetric short Au···S contacts into a zigzag polymer chain of the $(\cdots[A\cdots B\cdots A]^{3+}\cdots)_n$ type. The pairs of the $[ZnCl_4]^{2-}$ anions are joined by Cl(4)···O hydrogen bonds involving the outer-sphere water molecules and hydronium ions. The conditions for the regeneration of fixed gold were established by the study of the thermal behavior of complex **I** using the STA method.

EXPERIMENTAL

Sodium diisopropyl dithiocarbamate was synthesized by the reaction of carbon disulfide (Merck) and diisopropylamine (Merck) in an alkaline medium [10]. The starting binuclear complex chemisorbent was synthesized according to published data [11]. Both compounds were identified using the data of ^{13}C MAS NMR spectroscopy.

$Na\{S_2CN(iso\text{-}C_3H_7)_2\} \cdot 3H_2O$ (1 : 2 : 4), δ, ppm: 206.6 ($-S_2CN=$), 58.6, 51.3 (1 : 1, $=NCH=$), 21.7, 19.8 (3 : 1, $-CH_3$).

$[Zn_2\{S_2CN(iso\text{-}C_3H_7)_2\}_4]$, δ, ppm: 203.0 (50)*, 202.8, 199.7 (46)*, 199,6 (1 : 1 : 1 : 1, $-S_2CN=$); 61.8 (27)*, 59.8 (31)*, 52.6 (32)*, 50.8 (36)* (1 : 1 : 1 : 1, $=NCH=$); 21.9, 21.7, 21.5, 21.2, 20.5, 20.3, 20.2 (1 : 1 : 1 : 1 : 1 : 1 : 2, $-CH_3$) (* designate asymmetric $^{13}C-^{14}N$ doublets [12, 13], in Hz).

Synthesis of compound I. Polymer hexakis(N,N-diisopropyldithiocarbamato-S,S,S')trigold(III) hydronium-bis(tetrachlorozincate) hydrate (**I**) was synthesized by the interaction of freshly precipitated binuclear zinc diisopropyl dithiocarbamate [11] and a solution of $AuCl_3$ in 2 M HCl. The heterogeneous reaction including the chemisorption and partial ion exchange can be presented as follows:

$$3/2[Zn_2\{S_2CN(iso\text{-}C_3H_7)_2\}_4] + 3H[AuCl_4] + 2H_2O = H_3O[Au\{S_2CN(iso\text{-}C_3H_7)_2\}_2]_3[ZnCl_4]_2 \cdot H_2O + ZnCl_2 + 2HCl.$$

A solution of $AuCl_3$ (10 mL) in 2 M HCl containing gold (45.8 mg) was poured to zinc diisopropyl dithiocarbamate (100 mg), and the mixture was stirred for 1 h. The resulting lemon-yellow precipitate was filtered off, washed with water, dried on the filter, and dissolved in acetone. Yellow prismatic crystals of hydrated complex **I** suitable for X-ray diffraction analysis were obtained by the slow evaporation of the solvent.

^{13}C MAS NMR for compound **I**, δ, ppm: 192.0, 191.4, 189.6 (1 : 1 : 1, $-S_2CN=$); 60.0, 58.9, 57.3, 55.0, 54.3, 54.1 ($=NCH=$); 25.2, 24.8, 23.3, 22.5, 21.7, 21.2, 20.8, 20.5, 19.7, 19.0, 18.4, 17.8 ($-CH_3$).

Sorption of gold(III) was carried out in the static mode. A solution of $AuCl_3$ (10 mL) in 2 M HCl (concentration 7.05 mg/mL) was poured to portions of the starting chemisorbent (100 mg), and the mixture was magnetically stirred for 1 h. After the end of the reaction, 0.1-mL samples were taken from each solution for the determination of the residual gold concentration. The degree of extraction (S) was calculated by the formula

$$S = [(c - c_o)/c] \times 100\%,$$

where c and c_o are the initial and residual contents of gold in the solution, respectively. The amount of chemisorbed gold(III) is determined by this difference. The gold content in solutions was determined on a Hitachi atomic absorption spectrometer (class I, model 180-50).

^{13}C MAS NMR spectra were recorded on a CMX-360 spectrometer (Agilent/Varian/Chemagnetics InfinityPlus) with a working frequency of 90.52 MHz, a superconducting magnet ($B_0 = 8.46$ T), and a Fourier transform. Proton cross polarization was used. The decoupling effect was used to suppress $^{13}C^{-1}H$ interactions using a radiofrequency field at the resonance proton frequency [14]. A sample (~100 mg) was placed in a 4.0-mm ceramic rotor of ZrO_2. Magic angle spinning at a frequency of 5500–6000(1) Hz was used in ^{13}C MAS NMR measurements (scan number 1400–3200, duration of proton π/2 pulses 4.9 μs, $^1H-^{13}C$ contact time 2.5 ms, interval between pulses 3.0 s). The ^{13}C isotropic chemical shifts (δ scale in ppm) are relative to one of the components of crystalline adamantane used as an external standard [15] (δ = 38.48 ppm relative to tetramethylsilane [16]).

X-ray diffraction analysis of compound I was carried out from prismatic single crystals on a Bruker-Nonius X8 Apex CCD diffractometer (MoK_α radiation, λ = 0.71073 Å, graphite monochromator) at 100(2) K. The data were collected according to a standard procedure: φ and ω scan modes for narrow frames. An absorption correction was applied empirically (SADABS) [17]. The structure was solved by a direct method and refined by least squares (for F^2) in the full-matrix anisotropic approximation of non-hydrogen atoms. The positions of hydrogen atoms were calculated geometrically and included into refinement in the riding model. The oxygen atoms of the solvating H_2O molecule and H_3O^+ hydronium ion were randomly distributed between two positions with equal

populations (0.50). The hydrogen atoms in H_2O and H_3O^+ were not localized. The residual electron density was found in the expected range between −2.59 and 2.13 e/Å^3.

Data collection and editing and the refinement of unit cell parameters were performed using the APEX2 and SAINT programs [17]. Calculations on structure determination and refinement were performed using the SHELXTL program package [17]. The main crystallographic data and refinement results for structure **I** are listed in Table 1. Selected bond lengths and angles are given in Table 2. The coordinates of atoms, bond lengths, and angles were deposited with the Cambridge Crystallographic Data Centre (no. 908263; deposit@ccdc.cam.ac.uk or http://www.ccdc.cam.ac.uk).

Thermal behavior of compound I was studied by the STA method including the simultaneous detection of thermogravimetry (TG) and differential scanning calorimetry (DSC) curves on a STA 449C Jupiter instrument (NETZSCH) in capped corundum crucibles with a hole in the cap providing a vapor pressure of 1 atm in the course of the thermal decomposition of the sample. The heating rate was 5°C/min to 1100°C in argon. In addition, recording was carried out in aluminum crucibles to reveal more distinctly the heat effects at the initial stage. The weight of the samples ranged from 1.932 to 3.734 mg. The accuracy of the temperature measurement was ±0.7°C, and that of the weight change was $\pm 1 \times 10^{-4}$ mg. When recording the TG and DSC curves, the correction file was used as well as temperature sensitivity calibrations for the specified temperature program and heating rate. The independent determination of the melting point of compound **I** was carried out on a PTP(M) instrument (OAO Khimlaborpribor, Russia).

Table 1. Crystallographic data and the experimental and refinement parameters for structure **I**

Parameter	Value
Empirical formula	$C_{42}H_{89}N_6O_2S_{12}Cl_8Au_3Zn_2$
M	2100.15
Crystal system	Triclinic
Space group	$P\bar{1}$
a, Å	11.6473(3)
b, Å	12.2273(3)
c, Å	13.9410(4)
α, deg	92.5180(10)
β, deg	96.6120(10)
γ, deg	113.5800(10)
V, Å^3	1798.67(8)
Z	1
ρ_{calcd}, g/cm^3	1.939
μ, mm^{-1}	7.436
F(000)	1019
Crystal size, mm	0.18 × 0.08 × 0.06
Data collection in θ range, deg	1.83–30.14
Range of reflection indices	$-14 \le h \le 16$, $-16 \le k \le 6$, $-19 \le l \le 19$
Measured reflections	14242
Independent reflections	10358 ($R_{int} = 0.0146$)
Number of reflections with $I > 2\sigma(I)$	9062
Refinement variables	351
Goodness-of-fit	1.066
R factors on $F^2 > 2\sigma(F^2)$	$R_1 = 0.0257$, $wR_2 = 0.0596$
R factors on all reflections	$R_1 = 0.0328$, $wR_2 = 0.0615$
Residual electron density (min/max), e Å^{-3}	−2.589/2.134

RESULTS AND DISCUSSION

The restructuring of sorbent precipitates with a change in their color from white to stramineous and gradual deepening of the color to lemon-yellow were observed in the course of the interaction of the samples of the starting $[Zn_2\{S_2CN(iso\text{-}C_3H_7)_2\}_4]$ complex with the working solution of gold(III) chloride. These changes indicate the formation of new compounds in the system studied. The working solution was completely decolorized in parallel. The degree of extraction of gold from the solution was 99.23%. The sorption capacity of zinc diisopropyl dithiocarbamate calculated from the formation of the heteropolynuclear gold(III)–zinc complex was 471.2 mg of Au^{3+} per 1 g of the sorbent.

The ^{13}C MAS NMR spectrum (Fig. 1) of compound **I** isolated from the chemisorption system exhibits multicomponent groups of resonance signals in the region of the =NC(S)S–, =CH–, and –CH_3 groups (see Synthesis of compound **I**). The modeling of the spectrum from fragment to fragment made it possible to attribute the ^{13}C signals (1 : 1 : 1) to three nonequivalent =NC(S)S– groups, which indicates a complicated character of the structure of new compound **I** formed in the sorption system.

The molecular and supramolecular structures of complex **I** were determined by X-ray diffraction analysis to verify the above conclusions.

The structure of ionic complex **I** is shown in Fig. 2. The cationic part of the compound is presented by the hydronium ion and three complex ions $[Au\{S_2CN(iso\text{-}C_3H_7)_2\}_2]^+$ including the planar chromophores $[AuS_4]$ corresponding to the low-spin (intraorbital) dsp^2 hybrid state of gold (Fig. 3a). In the $[ZnCl_4]^{2-}$ anions, the metal atom exists in the tetrahedral environment of four chlorine atoms (Fig. 3b) (sp^3 hybrid state of the central atom).

Table 2. Selected bond lengths (*d*) and bond (ω) and torsion (φ) angles in structure **I***

Bond	*d*, Å	Bond	*d*, Å
	Cation A		
Au(1)–S(11)	2.3285(8)	N(11)–C(13)	1.505(4)
Au(1)–S(12)	2.3393(8)	C(12)–C(121)	1.517(5)
Au(1)–S(13)	2.3309(8)	C(12)–C(122)	1.525(5)
Au(1)–S(14)	2.3369(8)	C(13)–C(131)	1.524(5)
Au(1)···S(21)	3.5863(9)	C(13)–C(132)	1.520(5)
Au(1)···S(13)[a]	3.8119(8)	N(12)–C(14)	1.305(4)
S(11)–C(11)	1.738(3)	N(12)–C(15)	1.500(4)
S(12)–C(11)	1.742(3)	N(12)–C(16)	1.501(4)
S(13)–C(14)	1.739(3)	C(15)–C(151)	1.524(4)
S(14)–C(14)	1.742(3)	C(15)–C(152)	1.516(5)
N(11)–C(11)	1.311(4)	C(16)–C(161)	1.515(5)
N(11)–C(12)	1.502(4)	C(16)–C(162)	1.524(4)
	Cation B		
Au(2)–S(21)	2.3307(8)	N(21)–C(22)	1.499(4)
Au(2)–S(22)	2.3361(8)	N(21)–C(23)	1.505(4)
Au(2)···S(12)	3.6032(8)	C(22)–C(221)	1.516(5)
S(21)–C(21)	1.735(3)	C(22)–C(222)	1.521(5)
S(22)–C(21)	1.740(3)	C(23)–C(231)	1.523(5)
N(21)–C(21)	1.308(4)	C(23)–C(232)	1.525(5)
	Anion		
Zn(1)–Cl(1)	2.2840(10)	Zn(1)–Cl(3)	2.2601(10)
Zn(1)–Cl(2)	2.2445(10)	Zn(1)–Cl(4)	2.2706(17)
Angle	ω, deg	Angle	ω, deg
	Cation A		
S(11)Au(1)S(12)	75.04(3)	S(11)C(11)N(11)	126.7(3)
S(11)Au(1)S(13)	103.89(3)	S(12)C(11)N(11)	123.7(3)
S(11)Au(1)S(14)	172.60(3)	S(13)C(14)S(14)	109.46(17)
S(12)Au(1)S(14)	106.17(3)	S(13)C(14)N(12)	123.2(2)
S(12)Au(1)S(13)	178.60(3)	S(14)C(14)N(12)	127.3(2)
S(13)Au(1)S(14)	75.00(3)	C(11)N(11)C(12)	123.9(3)
Au(1)S(11)C(11)	87.91(11)	C(11)N(11)C(13)	118.8(3)
Au(1)S(12)C(11)	87.48(11)	C(12)N(11)C(13)	117.1(3)
Au(1)S(13)C(14)	87.29(11)	C(14)N(12)C(15)	119.4(3)
Au(1)S(14)C(14)	87.03(11)	C(14)N(12)C(16)	123.5(3)
S(11)C(11)S(12)	109.53(18)	C(15)N(12)C(16)	116.6(2)
	Cation B		
S(21)Au(2)S(22)	74.83(3)	S(21)C(21)N(21)	126.4(2)
S(21)Au(2)S(22)[b]	105.17(3)	S(21)C(21)N(21)	126.4(2)
S(21)Au(2)S(21)[b]	180.00(4)	S(22)C(21)N(21)	124.2(2)
S(22)Au(2)S(22)[b]	180.00(4)	C(21)N(21)C(22)	120.5(3)
Au(2)S(21)C(21)	88.04(11)	C(21)N(21)C(23)	123.3(3)
Au(2)S(22)C(21)	87.73(10)	C(22)N(21)C(23)	116.2(2)
S(21)C(21)S(22)	109.37(17)		
	Anion		
Cl(1)Zn(1)Cl(2)	114.59(4)	Cl(2)Zn(1)Cl(3)	113.77(4)
Cl(1)Zn(1)Cl(3)	109.92(4)	Cl(2)Zn(1)Cl(4)	105.61(5)
Cl(1)Zn(1)Cl(4)	103.35(5)	Cl(3)Zn(1)Cl(4)	108.84(5)

Table 2. (Contd.)

Angle	φ, deg	Angle	φ, deg
Cation A			
Au(1)S(11)S(12)C(11)	−177.9(2)	S(12)C(11)N(11)C(12)	−171.3(2)
Au(1)S(13)S(14)C(14)	167.7(2)	S(12)C(11)N(11)C(13)	3.7(4)
S(11)Au(1)C(11)S(12)	−178.1(2)	S(13)C(14)N(12)C(15)	0.5(4)
S(13)Au(1)C(14)S(14)	168.8(2)	S(13)C(14)N(12)C(16)	−170.9(2)
S(11)C(11)N(11)C(12)	11.2(5)	S(14)C(14)N(12)C(15)	179.0(2)
S(11)C(11)N(11)C(13)	−173.8(2)	S(14)C(14)N(12)C(16)	7.5(4)
Cation B			
Au(2)S(21)S(22)C(21)	−178.5(2)	S(21)C(21)N(21)C(23)	5.4(4)
S(21)Au(2)C(21)S(22)	−178.6(2)	S(22)C(21)N(21)C(22)	3.4(4)
S(21)C(21)N(21)C(22)	−176.1(2)	S(22)C(21)N(21)C(23)	−175.1(2)

* Symmetry transforms: [a] $2-x, -y, 1-z$; [b] $2-x, 1-y, 1-z$.

In each gold(III) cation, the both dithiocarbamate ligands are characterized by a nearly S,S'-isobidentate coordination mode (Au–S 2.3285–2.3393 Å), due to which two four-membered metallocycles $[AuS_2C]$ joined by the common gold atom are formed. The cycles are small: the Au···C 2.842–2.857 Å) and S···S 2.836–2.843 Å interatomic distances are substantially shorter than the sums of the van der Waals radii of the corresponding pairs of the atoms (Au, C 3.36 Å and 2S 3.60 Å [18–20]). These data indicate a high general degree of binding of the atoms in the bicyclic group $[Au(S_2C)_2]$ due to the high concentration of the π-electron density delocalized inside the sterically strained four-membered metallocycles. The cycles are almost planar, and only one of them in the noncentrosymmetric Au(1) cation exhibits a significant tetrahedral distortion (torsion angles AuSSC 167.7° and SAuCS 168.8° (Table 2)). The gold polygons $[AuS_4]$ are rectangles (the deviation of the S···S···S angles from 90° does not exceed 1°) with the S···S sides equal to 2.836–2.843 and 3.669–3.739 Å (intraligand and interligand distances, respectively). The N–C(S)S bonds (1.305–1.311 Å) in the Dtc groups are substantially shorter than N–CH (1.499–1.505 Å) due to the mesomeric effect. For the same reason, the atoms in the C_2N–C(S)S groups are nearly coplanar, and the maximum deviation from the plane is characteristic of the C(12) and C(16) atoms (see the values of the corresponding torsion CNCS angles in Table 2).

Of three complex cations $[Au\{S_2CN(iso\text{-}C_3H_7)_2\}_2]^+$ of the discussed heteropolynuclear compound, two noncentrosymmetric cations (cations A

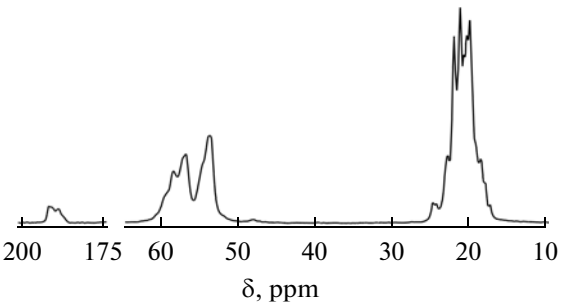

Fig. 1. ^{13}C MAS NMR spectrum of complex **I** (scan number/spinning frequency 3200/6000).

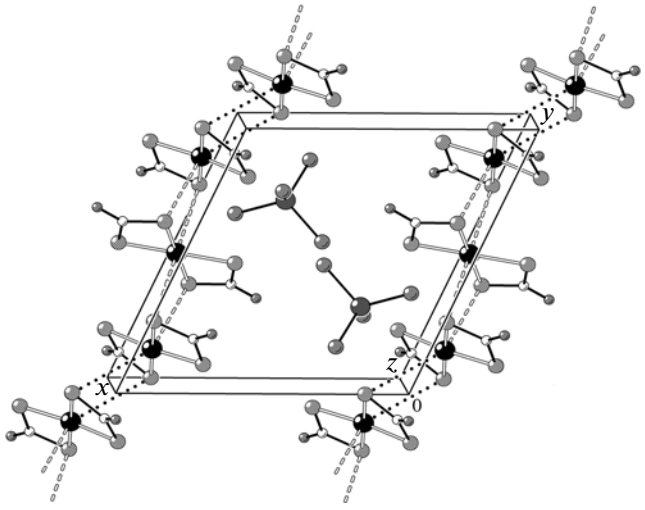

Fig. 2. Projection of the $(H_3O[Au_3\{S_2CN(iso\text{-}C_3H_7)_2\}_6][ZnCl_4]_2 \cdot H_2O)_n$ structure (**I**) on the *xy* plane. Secondary bonds Au···S are shown by double dashed lines; short contacts between the trinuclear structural fragments are designated by dotted lines. The *iso*-C_3H_7 groups, H_3O^+ cations, and H_2O molecules are omitted.

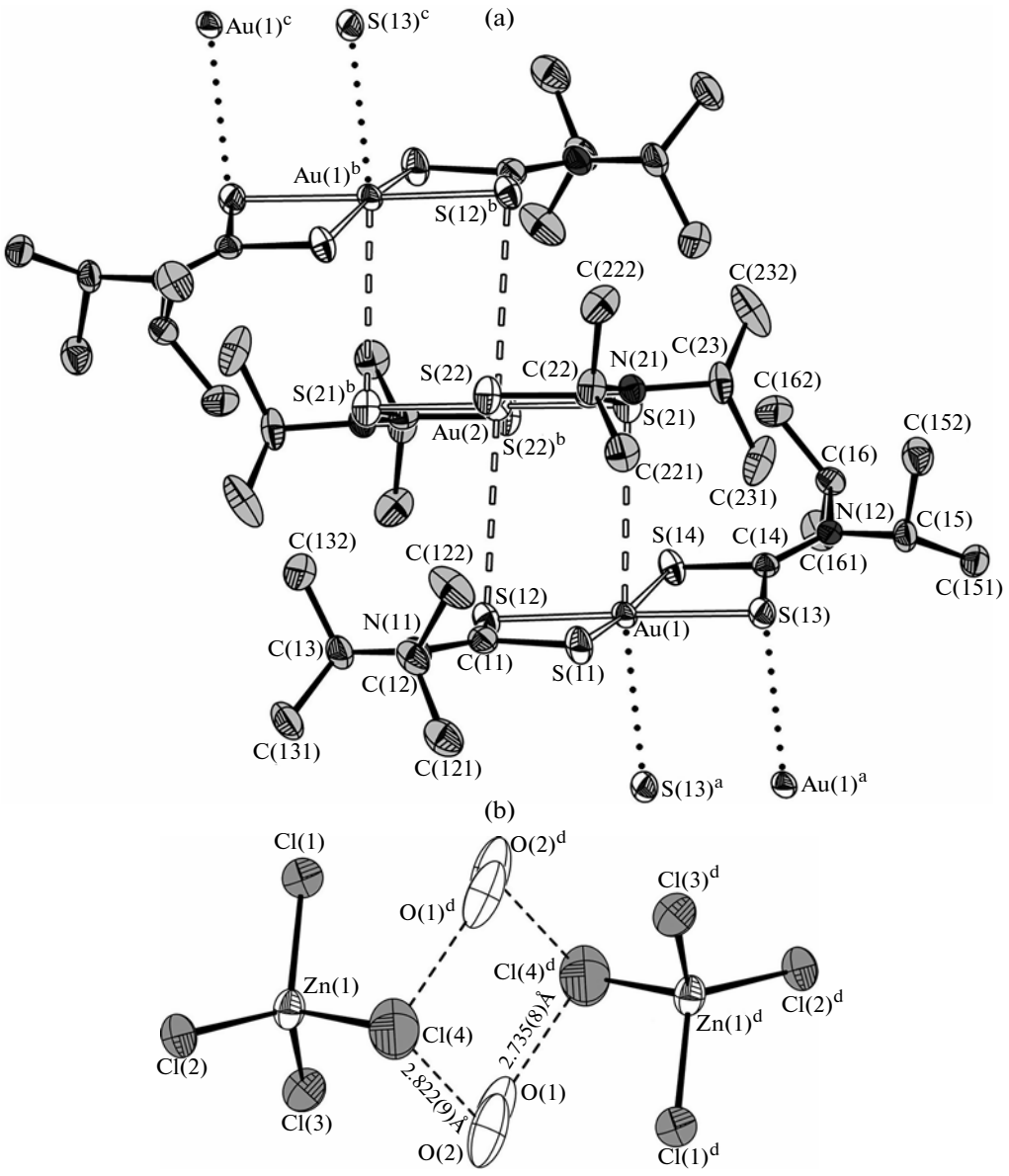

Fig. 3. (a) Trinuclear structural fragment $[Au_3\{S_2CN(iso\text{-}C_3H_7)_2\}_6]^{3+}$. Intercationic secondary Au···S bonds are shown by double dashed lines; short contacts between the trinuclear structural fragments are designated by dotted lines. (b) Mutual spatial arrangement of the $[ZnCl_4]^{2-}$ anions, H_3O^+ cations, and H_2O molecules; hydrogen bonds are shown by dashed lines. Ellipsoids with the 70% probability (symmetry transforms: [c] $x, 1 + y, z$; [d] $1 - x, 1 - y, 2 - z$).

with the Au(1) atom) are structurally nonequivalent with respect to the third centrosymmetric one (cation B including the Au(2) atom) (Fig. 3a, Table 2). Thus, as expected from the ^{13}C MAS NMR data, compound **I** includes three (1 : 1 : 1) structurally nonequivalent Dtc ligands. The structural similarity of complex cations A and B is consistent with their nonequivalence, and the character of the structural differences observed (Table 2) makes it possible to classify them as conformational isomers.

The further structural ordering of complex **I** at the supramolecular level occurs due to relatively weak secondary Au···S bonds[2] between the isomeric cations $[Au\{S_2CN(iso\text{-}C_3H_7)_2\}_2]^+$. Each centrosymmetric cation B forms a pair of nonequivalent secondary

[2] The concept of secondary bonds was proposed [21] for the description of interactions characterized by distances comparable with the sums of the van der Waals radii of the corresponding atoms.

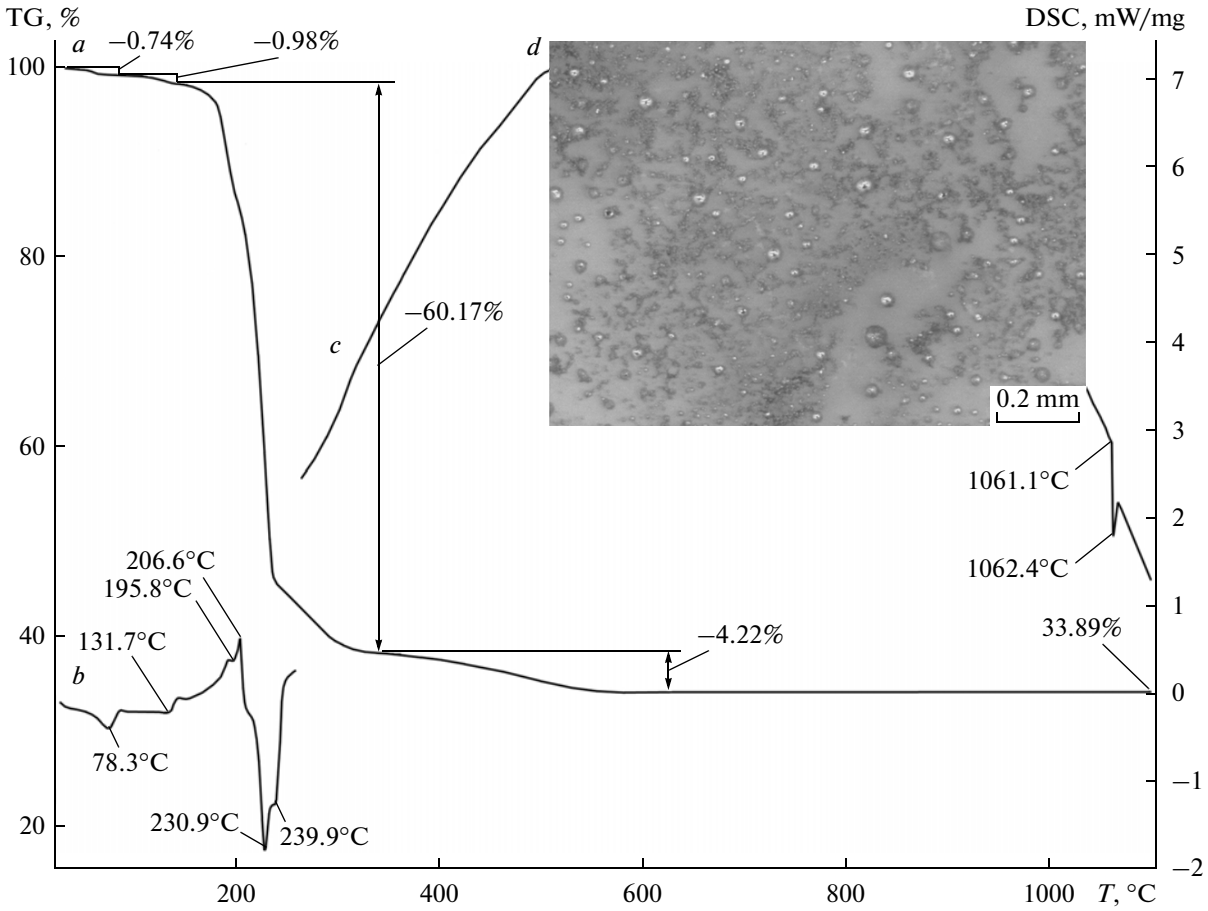

Fig. 4. (*a*) TG and (*b*, *c*) DSC curves for complex **I** (*b* is the low-temperature (below 280°C) DSC fragment of the curve recorded in an aluminum crucible); (*d*) enlarged fragment of the crucible bottom at the thermolysis completion.

bonds with each of two adjacent noncentrosymmetric cations A: Au(2)···S(12), Au(2)···S(12)^{b} 3.6032 and Au(1)···S(21), Au(1)^{b}···S(21)^{b} 3.5863 Å. The length of these bonds somewhat exceeds the sum of the van der Waals radii of the gold and sulfur atoms (3.46 Å) [18–20]. As a result, trinuclear structural fragments $[Au_3\{S_2CN(iso\text{-}C_3H_7)_2\}_6]^{3+}$ of the [A···B···A] type are formed (Au(1)···Au(2) 4.129 Å, angle Au(1)Au(2)Au(1) 180°) in which cations A are antiparallel (Fig. 3a). The trimers formed are joined by pairs of short contacts between cations A: Au(1)···S(13)^{a} and Au(1)^{a}···S(13) 3.8119 Å. This leads to the formation of zigzag polymer chains $(\cdots[A\cdots B\cdots A]\cdots)_n$ along the crystallographic axis *y*. The Au(1)···Au(1) distance is 4.494 Å, and the Au(1)···Au(1)···Au(2) angle is 145.43°.

The complex anions $[ZnCl_4]^{2-}$, outer-sphere water molecules, and hydronium ions are localized between the polymer chains (Figs. 2 and 3b). Two adjacent $[ZnCl_4]^{2-}$ anions are joined by hydrogen bonding involving the chlorine atom, solvating H_2O molecule, and H_3O^+ ion (Fig. 3b). The Cl(4)^{d}···O(1) 2.735 and Cl(4)···O(2) 2.822 Å distances are substantially shorter than the sums of the van der Waals radii of the oxygen and chlorine atoms (3.27 Å) [18–20]. Probably, the positively charged H_3O^+ ion forms a stronger hydrogen bond with the negatively polarized chlorine atom than the water molecule does [22]. Therefore, it seems reasonable that the O(1) oxygen atom is in the composition of the hydronium ion.

The conditions for the regeneration of fixed gold were established by the STA study of the thermal behavior of compound **I** (parallel recording of the TG and DSC curves) under an argon atmosphere. The TG curve shows the multistage mass loss by the studied complex (Fig. 4*a*). At the initial stage of thermolysis (below ~145°C), the TG curve detects two small mass loss steps of 0.74 and 0.98% (totally 1.72%) corresponding to the two-step dehydration of the complex (calcd. 0.86 × 2 = 1.72%). The main mass loss (60.17%) is presented by the next steeply descending region of the TG curve with several inflection points indicating the consecutive occurrence of several processes. The stage discussed (145–340°C) is related to the reduction of metallic gold (in the cation), the lib-

eration of zinc chloride, and its partial transformation into ZnS (in the anion).[3] The completing third stage (340–600°C) is caused by the evaporation of $ZnCl_2$ (mp = 317°C and bp = 733°C [24]). The considerable content of sulfur (18.32%) in the complex, which manifests a high affinity to gold, suggests that the direct precursor of reduced gold is Au_2S (T_{decomp} = 240°C [24]). This is indirectly confirmed by the corresponding inflection point in the TG curve.

The residual weight at 1100°C (33.89% of the initial value) exceeds the expected one for reduced gold (calcd. 28.14%) by 5.75%. When assigning this excessive weight to ZnS (sublimes only at 1185°C [24]), one should take into account that its formation requires 61.96% zinc existing in the complex. Therefore, 38.04% zinc remained in the form of $ZnCl_2$. The corresponding amount of zinc chloride is 4.94% of the initial weight of the complex, which is rather close to the experimentally observed mass loss at the third stage (4.22%). After the crucible was opened, gold balls (from 0.004 to 0.05 mm in diameter) and zinc sulfide colored in reddish-brown due to the incorporation of finely dispersed particles of reduced gold were found on the bottom (Fig. 4*d*).

The low-temperature region of the DSC curve contains three weakly pronounced endotherms (with extremes at 78.3, 131.7, and 195.8°C) corresponding to two dehydration steps of the complex followed by melting of its dehydrated form (Fig. 4*b*). (The phase transition was found in the temperature range from 188 to 190°C by the determination of the melting point of complex **I** pressed in a glass capillary.) The next region of the DSC curve corresponding to the active thermolysis zone shows several overlapped heat effects, indicating a complicated character of the thermolysis. The high-temperature region includes the endotherm of gold melting (Fig. 4*c*): the extrapolated melting point is 1061.1°C.

ACKNOWLEDGMENTS

The authors are grateful to A.I. Smolentsev (Nikolaev Institute of Inorganic Chemistry, Siberian Branch, Russian Academy of Sciences, Novosibirsk) for X-ray diffraction analyses and to O.N. Antzutkin (Luleä University of Technology, Sweden) for the kindly presented possibility of recording the ^{13}C MAS NMR spectra.

This work was supported by the Presidium of the Russian Academy of Sciences (program for support of basic research "Development of Methods for Synthesis of Chemical Substances and Preparation of New Materials," project no. 12-I-P8-01) and the Presidium of the Far East Branch of the Russian Academy of Sciences (project nos. 12-III-A-04-040 and 13-III-B-04-041).

[3] The formation of metal sulfides due to the thermolysis of the complexes bearing sulfur-containing ligands was substantiated from the thermodynamic positions [23].

REFERENCES

1. Rodina, T.A., Ivanov, A.V., Gerasimenko, A.V., et al., *Polyhedron*, 2012, vol. 40, no. 1, p. 53.
2. Rodina, T.A., Filippova, T.S., Ivanov, A.V., et al., *Russ. J. Inorg. Chem.,* 2012, vol. 57, no. 11, p. 1490.
3. Ivanov, A.V., Zinkin, S.A., Gerasimenko, A.V., and Sergienko, V.I., *Russ. J. Coord. Chem.*, 2011, vol. 37, no. 6, p. 452.
4. Loseva, O.V., Rodina, T.A., Ivanov, A.V., et al., *Russ. J. Coord. Chem.*, 2011, vol. 37, no. 12, p. 897.
5. Ivanov, A.V., Zinkin, S.A., Sergienko, V.I., et al., *Russ. J. Inorg. Chem.*, 2011, vol. 56, no. 3, p. 409.
6. Ivanov, A.V., Sergienko, V.I., Gerasimenko, A.V., et al., *Russ. J. Coord. Chem.*, 2010, vol. 36, no. 5, p. 353.
7. Loseva, O.V., Ivanov, A.V., Gerasimenko, A.V., et al., *Russ. J. Coord. Chem.*, 2010, vol. 36, no. 1, p. 3.
8. Ivanov, A.V., Loseva, O.V., Gerasimenko, A.V., and Sergienko, V.I., *Dokl. Phys. Chem.*, 2009, vol. 426, no. 3, p. 92.
9. Rodina, T.A., Ivanov, A.V., and Loseva, O.V., Abstracts of Papers, *VII Vseros. konf. po khimii poliyadernykh soedinenii i klasterov* (VII All-Russian Conf. on the Chemistry of Polynuclear Compounds and Clusters), Novosibirsk, 2012, p. 295.
10. Byr'ko, V.M., *Ditiokarbamaty* (Dithiocarbamates), Moscow: Nauka, 1984.
11. Miyamae, H., Ito, M., and Iwasaki, H., *Acta Crystallogr., Sect. B: Struct. Sci.*, 1979, vol. 35, no. 6, p. 1480.
12. Hexem, J.G., Frey, M.H., and Opella, S.J., *J. Chem. Phys.*, 1982, vol. 77, no. 7, p. 3847.
13. Harris, R.K., Jonsen, P., and Packer, K.J., *Magn. Reson. Chem.*, 1985, vol. 23, no. 7, p. 565.
14. Pines, A., Gibby, M.G., and Waugh, J.S., *J. Chem. Phys.*, 1972, vol. 56, no. 4, p. 1776.
15. Earl, W.L. and VanderHart D.L., *J. Magn. Reson.*, 1982, vol. 48, no. 1, p. 35.
16. Morcombe, C.R. and Zilm, K.W., *J. Magn. Reson.*, 2003, vol. 162, no. 2, p. 479.
17. *Bruker. APEX2 (version 1.08), SAINT (version 7.03), SADABS (version 2.11) and SHELXTL (version 6.12)*, Madison (WI, USA): Bruker AXS Inc., 2004.
18. Pauling, L., *The Nature of the Chemical Bond and the Structure of Molecules and Crystals*, London: Cornell Univ., 1960.
19. Bondi, A., *J. Phys. Chem.*, 1964, vol. 68, no. 3, p. 441.
20. Bondi, A., *J. Phys. Chem.,* 1966, vol. 70, no. 9, p. 3006.
21. Alcock, N.W., *Adv. Inorg. Chem. Radiochem.*, 1972, vol. 15, no. 1, p. 1.
22. Fulton, J.L. and Balasubramanian, M., *J. Am. Chem. Soc.*, 2010, vol. 132, no. 36, p. 12597.
23. Razuvaev, G.A., Almazov, G.V., Domrachev, G.A., et al., *Dokl. Akad. Nauk SSSR*, 1987, vol. 294, no. 1, p. 141.
24. Lidin, R.A., Andreeva, L.L., and Molochko, V.A., *Spravochnik po neorganicheskoi khimii* (Reference Book in Inorganic Chemistry), Moscow: Khimiya, 1987.